Strojniški vestnik - Journal of Mechanical Engineering 68(2022)6, 439-448
© 2022 The Authors. CC BY 4.0 Int. Licensee: SV-JME
DOI:10.5545/sv-jme.2022.98
Original Scientific Paper
Received for review: 2022-03-05
Received revised form: 2022-04-26
Accepted for publication: 2022-05-23

Determination of Limiting Dome Height (LDH) Values for Inconel 718 Alloy Sheet Using FEA and a Hemispherical Punch Method

Kanmani Ganesan* – Saravanan Sambasivam – Rajesh Ramadass
PSG College of Technology, Department of Production Engineering, India

In a uniaxial tensile test, the material properties of Inconel 718 alloy sheet, such as yield strength, ultimate tensile strength, percentage of elongation, normal anisotropy, planar anisotropy, strain hardening exponent and the strength coefficient were determined in the longitudinal, diagonal, and transverse rolling directions. The main aim of this research is focused on the determination of limiting dome height (LDH) values for Inconel 718 alloy sheet of 1 mm thickness through experiments and finite element analysis using a hemispherical punch method. A limit curve was established through experimentation, which ensures a safe working region for 1 mm thick Inconel 718 sheet at room temperature. Scanning electron microscope (SEM) analysis of 100 mm and 120 mm width specimens indicated smooth surfaces and ductile fractures. The examination of 140 mm and 160 mm width specimens showed rough surfaces and shear-ductile failures. In finite element analysis, Barlat-89 yield criterion was used to obtain the limiting dome height (LDH) values and strain distribution in the specimen using ABAQUS6.1. A close relationship with minor deviation was observed between the experimental LDH values and finite element analysis results. The chemical composition of the fractured sheet examined using energy dispersive spectrum (EDS) analysis was similar to the results observed with an X-ray fluorescence (XRF) technique conducted on the Inconel 718 alloy sheet before failure. The approach presented in this work can be applied to obtain the LDH values of researched material focused.

Keywords: Inconel 718 alloy sheet, uniaxial tensile test, hemispherical punch method, LDH values, SEM, EDS

Highlights

- *The mechanical properties of Inconel 718 alloy sheet of 1mm thickness were obtained in different rolling directions.*
- *The percentage of elongation was high (47.6 %) in the rolling direction compared to other transverse directions.*
- *The strain hardening (n) is found to be 0.34, which indicates good stretch ability and formability.*
- *The strain limit obtained is the safe region where the material is susceptible to plastic deformation without failure.*
- *The LDH values obtained from ABAQUS6.1 and experimental results were in good agreement. The error was found to be less than 5 %.*

0 INTRODUCTION

The usage of superalloys is increasing in aerospace and defence applications. Inconel is a nickel-chromium alloy with exceptional corrosion and oxidation resistance that is used at extreme environments. The transformation of sheet metal into desired shapes without deformation is considered as the measure of formability of a material. The sheet metal formability is evaluated using different methods, such as the Keeler test, Hecker test, Markiniak test, Nakizima test, and Hasek test. Gupta and Kumar **[1]** applied a Hecker simplified technique for the formability of galvanized interstitial free sheets. The forming limit diagram (FLD) has been evaluated experimentally using a hemispherical punch method. Pérez Caro et al. **[2]** determined that among the various nickel-based superalloys, the properties of Inconel 718 alloys sheets have attracted the attention of researchers for manufacturing sheet metal components. Reed **[3]** and Anderson et al. **[4]** discussed sheet metal forming processes that are commonly used in industries and compared them to other manufacturing process as the grain orientation remains unaffected after processing the material. The authors **[4]** also reported that Inconel 718 alloy sheet is one of the hardest alloys in nickel-chromium-iron-based superalloy family widely used in the form of sheet metal for fabricating fuel cells, outer casings, heat exchanger devices, fuel tanks, and various structures of space and aircraft vehicles. Sajun Prasad et al. **[5]** reported that the formability of the material in the sheet metal forming process is evaluated using FLD, and the trend line is obtained as a plot between circumferential and radial strain measurement. A rigid hemispherical punch and die set up was used to obtain the FLD. It indicated the maximum strain that the material can withstand before failure. Banabic al. **[6]** observed that the experimental determination of FLD is a time-consuming process, which has led to the development of numerical models and computational methods. Jayahari et al. **[7]** predicted the mechanical properties of Inconel 718 alloy sheet at sub-zero temperatures in different rolling directions using artificial neural networks

*Corr. Author's Address: PSG College of Technology, Department of Production Engineering, India, gvmani.engr@gmail.com

(ANN). Djavanroodi and Derogar [8] investigated the strain distribution in the forming of Ti6A14 alloy and Al6061-T6 alloy sheets; the impact of factors on the FLD was also evaluated and simulated using ABAQUS. Narayanasamy and Narayanan [9] obtained the experimental FLD for interstitial free (IF) steel of different thicknesses by press forming. Also, the SEM analysis of fractured test specimens in a uniaxial test showed ductile fractures. Badr et al. [10] explored various yield criteria and hardening rules to convert the forming limit diagram to a forming limit stress diagram. It was found that the Barat-89 and Hosford-79 material models provided extremely high accuracy values against the experimental results obtained using the forming limit diagram. Toshniwal et al. [11] studied the mechanical properties of Ti-6A1-4V using tensile test and obtained the FLD of the material using a stretch forming test. Sudarsanetal. [12] determined the mechanical properties of SS304 in three different rolling directions and studied the influence of parameters on the limiting strain. Rahmaanet al. [13] examined the strain rate influence on flow stress and anisotropy for the sheet metal alloys DP600, TRIP780 and AA5182-O. These materials exhibit no significant dependence of anisotropy and strain rate in the tensile test. Li et al. [14] studied the strain rate influence on the mechanical properties, fracture mechanism of DP780 dual-phase steel was investigated; it was found that the micro-cracks and voids increased with increases in the strain rate. Mahalle et al. [15] found that the FLD for precipitate hardened Inconel 718 alloy at various temperatures from room temperature to 700° using Nakazima test. The author also emphasized that the theoretical models proposed for FLD prediction are the Swift model, Hill model, and M-K model. The application of these models for formability prediction is a time-consuming process. The finite element method for the prediction of LDH values is urgently needed in the sheet metal industry. Finite element analysis reduces the costs incurred by the trial-and-error method of sheet metal forming. Paul [16] declared that FLD is extremely sensitive on strain paths. The yield criterion selection had a significant impact on the results of a stress-based forming limit diagram. Paul [17] developed a model to predict the FLC of steel sheets from the simple tensile properties of the material. Paul [18] identified minor deviations of FLC using the International Organization for Standardisations (ISO), time dependant, slope, and flat valley methods. The detailed review of journal articles quoted in the above discussion [1] to [18] revealed that only very minimum work was done in the topic of "LDH determination for Inconel 718 alloy sheet at room temperature".

Therefore, the proposed work discusses the new findings related to the gap identified in the literature study. The chemical composition of Inconel 718 alloy sheet was found using XRF. The mechanical properties of the sheet were obtained in different rolling directions using a uniaxial tensile test. The LDH values of 1 mm thick Inconel 718 alloy sheet were determined by experimentation and finite element analysis using the hemispherical punch method. SEM and EDS analysis of the fracture specimen is also presented.

1 MATERIALS AND METHODS

The workflow process chart is indicated in Fig. 1. The Inconel 718 alloy sheet was tested for chemical composition using the XRF technique. The sheet was subjected to uniaxial tensile testing, and the mechanical properties were determined in different rolling directions. The specimens were prepared as per Hecker's simplified technique; experimental LDH values and FLD for the Inconel 718 alloy sheet were obtained using the hemispherical punch method. The test results obtained from uniaxial tensile test were provided as input to ABAQUS 6.1. The strain distribution along with simulated LDH values was obtained. The LDH values obtained through experiment and Finite Element Analysis (FEA) simulation results were compared. If the results are not in agreement, the FEA-based simulation is repeated in ABAQUS 6.1. If the results are in close agreement, then the results of the work are summarized in the conclusion.

1.1 Chemical Composition and Microstructure

Inconel 718 alloy sheet (1 mm thickness) was subjected to chemical composition testing using an X-ray fluorescence (XRF) technique. The elements Cr, Mo, Fe, Al, and Ti are especially important for increasing solid solution strengthening and corrosion resistance; the count of niobium helps to increase the creep strength in the deep-drawing application. The chemical composition of Inconel 718 alloy sheet is shown in Table 1. The alloy specimens were prepared by electrically etching them. The polishing was performed using oxalic acid and water in a proportion of 1:10 for studying the microstructure with an optical microscope.

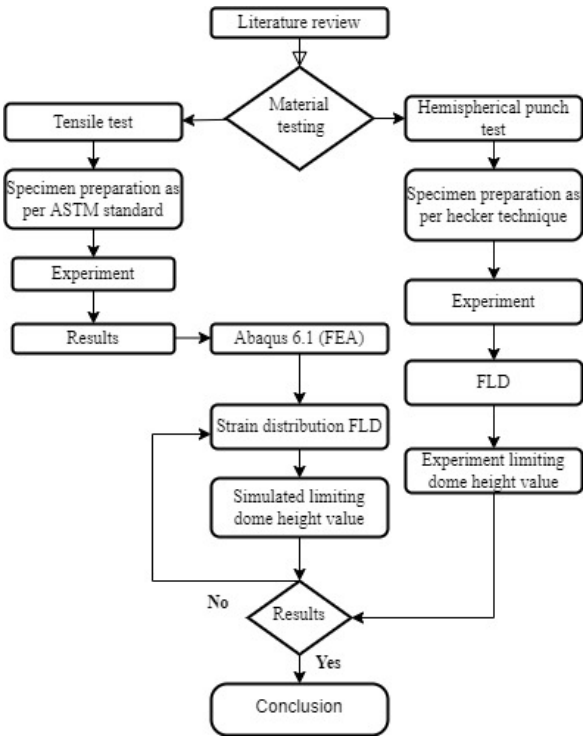

Fig. 1. *Process flow chart*

Table 1. *Chemical composition of Inconel 718 alloy sheet*

Element	Ni	Cr	Fe	Nb	Mo	Ti	Al
%	53.2	19.5	18.2	4.8	3.0	1.8	1.2

Microstructure obtained from optical microscope, shown in Fig. 2. indicates grain size of 7.5 µm with morphology variations in rolling direction, transverse and diagonal direction.

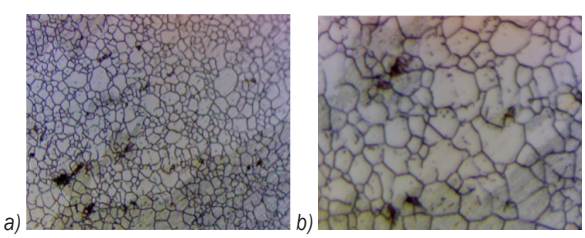

Fig. 2. *Microstructure of Inconel 718 alloy sheet before deformation; a) mag:200×, and b) mag:500×*

1.2 Tensile Test

The specimen the or uniaxial tensile test is prepared as per ASTM E8M standard [19] by wire-cut electrical discharge machining (WEDM) shown in Fig. 3.

The specimen was prepared using WEDM to obtain good surface finish and tight tolerance in Inconel 718 alloy sheets. The specimens were prepared in three different directions: parallel (0 degree), diagonal (45 degree) and perpendicular (90 degree) rolling direction as indicated in Fig. 4. The uniaxial test was carried out at a constant crosshead speed of 2 mm/min.The tensile test was per formed in a Zwick/ Roelltensile testing machine of 100 kN (UTM). The constants representing the material behaviour in a range of the plastic region is determined using the true stress-strain curves.

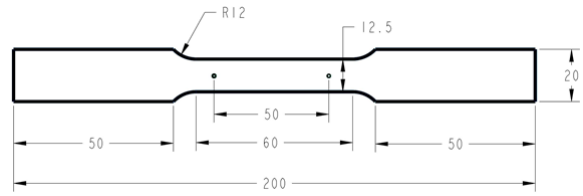

Fig. 3. *Tensile specimen as per ASTM E8M*

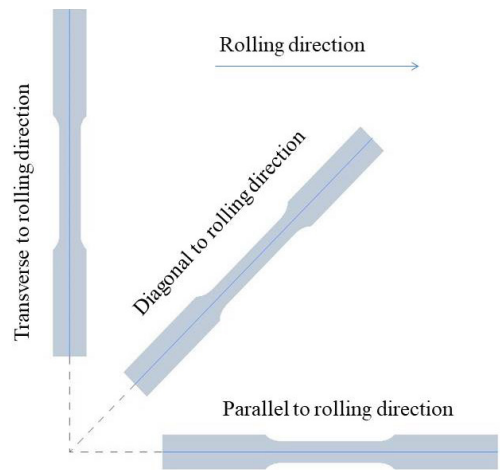

Fig. 4. *Tensile samples in different rolling direction*

The strain-hardening exponent (n) of materials is characterized by Hollomon's power law, and it plays an important role in formability, as shown in Eq. (1). The Lankford coefficient (r-value), normal (R) and planar (ΔR) anisotropy of the sheet materials are calculated with Eqs. (2) to (4).

$$\sigma = K\varepsilon^n, \tag{1}$$

$$r = \frac{\partial w}{\partial t} = \frac{\ln\left(\frac{w_f}{w_0}\right)}{\ln\left(\frac{l_0 w_0}{l_f w_f}\right)}, \tag{2}$$

$$R = \frac{r_0 + r_{45} + r_{90}}{4}, \tag{3}$$

$$\Delta R = \frac{r_0 - 2r_{45} + r_{90}}{2}, \tag{4}$$

where K *is* the strength coefficient, ε *true strain,* w_f is final width, w_O initial width, l_f final length, l_O initial length of sheet.

1.3 Forming Limit Diagram (FLD)

FLD is an important parameter index that describes the maximum limit of principal strain that the material can withstand before failure. Limiting strains at necking and fracture are determined using forming limit diagram and fracture limit curve in sheet metal forming. Kotkunde et al. [20] prepared the specimens using Hecker's simplified technique for experimental determination of FLD in Ti-6Al-4V alloy. Thus, in this work, the specimens of the Inconel 718 alloy sheet for experimental FLD were also prepared with Hecker's simplified technique.

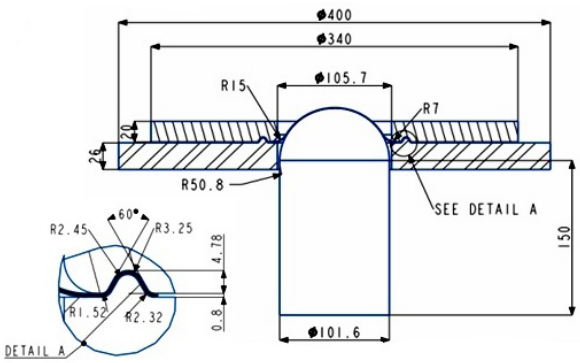

Fig. 5. *Schematic model of hemispherical punch test*

The FLD for Inconel 718 alloy sheet is obtained using a specifically designed and fabricated hemispherical punch, blank holder, and die. Fig. 5 shows a schematic drawing of the hemispherical punch die setup. Fig. 6 indicates the 3D model and the details of the individual parts. Three steps are followed during the experimental procedure: grid marking, punch-stretching of a grid marked sheet, and strain measurement of a deformed specimen.

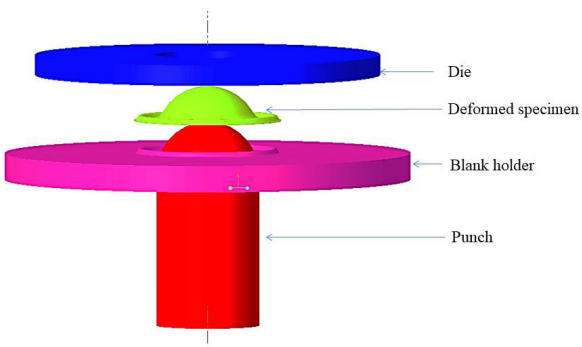

Fig. 6. *3D Model of forming die setup*

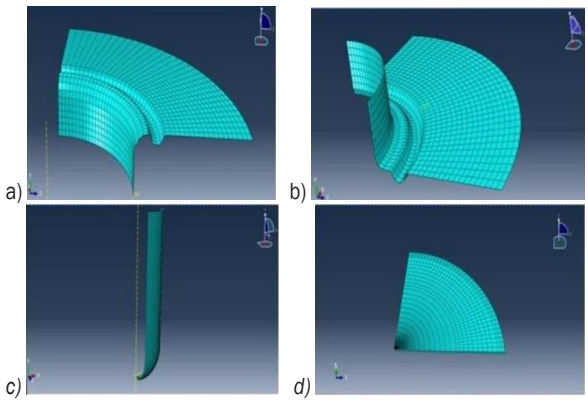

Fig. 7. *Meshing of components in ABAQUS 6;*
a) die meshed eight node linear brick element,
b) blank holder meshed four node linear tetrahedron element,
c) punch meshed four node linear tetrahedron element, and
d) sheet meshed eight node linear brick element

1.4 Finite Element Analysis

The components of the setup (e.g., die, blank holder, and hemispherical punch) were modelled based on the reference [9]. The numerical simulation of the stretch forming process was performed using ABAQUS6.1. The punch, die, and blank holder were modelled as discrete rigid bodies, while the sheet metal was modelled as a deformable material. Explicit surface-to-surface contact was established between the punch and blank, the blank and blank holder, and between the blank and die. An eight-node linear brick element (C3D8R) was used as a meshing element for the die, punch, and blank holder. Four-node linear tetrahedron elements were used as meshing elements for the blank. The punch is assigned the movement only in the z direction. The degrees of freedom in x, y and z directions were arrested for the rest of the components in the die. A draw bead was created on the die to inhibit the material flow from the flange part where the blank holding force was applied in the z-direction. The quarter model is considered to reduce the simulation time; the meshing of components is shown in Fig.7. A Barlat-89 yield function material model is shown in Eq. (5) and the terms k_1 and k_2 are mentioned in Eq. (6). The experimentally determined material properties (i.e., yield strength, ultimate tensile strength, percentage of elongation, normal anisotropy, planar isotropy, strain hardening exponent and Poisson's ratio) were given as inputs for the material and are simulated by ABAQUS 6.1.

$$a\left|k_1+k_2\right|^M+b\left|k_1-k_2\right|^M+c\left|2k_2\right|^M=2\sigma_e{}^M, \quad (5)$$

$$k_1 = \frac{(\sigma_x - h_{\sigma y})}{2}; \quad k_2 = \left(\frac{\sigma_x - h_{\sigma y}}{2} + p^2 \tau_{xy}^2 \right)^2, \quad (6)$$

where a, b, c, hand p are anisotropic parameters, k_1 and k_2 coefficients, M invariants of the stress, and σ_x effective stress.

1.5 SEM Fracture Analysis

The micro-structural changes of sheet metal are examined using SEM. The behaviour of the sheet metal is predicted from SEM images. The main aim is to understand the limits and behaviour of the material and possible causes of failure under biaxial strain conditions. Narayanasamy and Narayanan [21] used SEM fractography to understand the fracture behaviour and formability of interstitial free steel. In this work, the SEM fractography was used to examine the fracture surface of an Inconel 718 alloy sheet obtained from a hemispherical punch method.

2 RESULTS AND DISCUSSION

2.1 Tensile Test Results

Mechanical properties, such as yield strength, ultimate tensile strength, elongation, anisotropy parameters, strain hardening and strength coefficient of Inconel 718 alloy sheet metal are determined in three different rolling directions; the results of the tests are shown in Tables 2 and 3.

Table 2. *Tensile properties of Inconel alloy sheet*

Direction	YS [N/mm²]	UTS [N/mm²]	Total % of elongation
0°	512.1	820.9	47.6
45°	545.3	942.5	43.9
90°	614.6	931.3	45.1

Table 3. *Anisotropy properties & strain hardening exponent of Inconel alloy sheet*

Direction	r values	R	ΔR	n	K
0°	1.18	1.03	–0.04	0.33	2022
45°	0.97	0.97		0.31	1564
90°	0.91	0.94		0.32	1522

where YS is yield strength, UTS ultimate tensile strength, r anisotropy parameter, R normal anisotropy, ΔR planar anisotropy, n strain hardening exponent, and K strength coefficient.

Strain hardening n is found to be 0.33, which indicates good stretch ability and formability, whereas normal anisotropy r is 1.02, which shows resistance to thinning while drawing. The total elongation is found to be maximum in the longitudinal rolling direction compared to the diagonal and traverse rolling directions. Prasad al. [19] and Ravi Kumar and Swaminathan [22] reported similar results in Inconel 718 alloy sheets and aluminium alloys. The Inconel 718 has a negative planar anisotropy of –0.04 which can result in earing in the diagonal rolling direction.

True stress and true strain values, engineering stress and strain values are plotted and are shown in Fig. 8. Based on the observed values, the Inconel 718 alloy sheet percentage of elongation and strength were found to be good in the rolling direction.

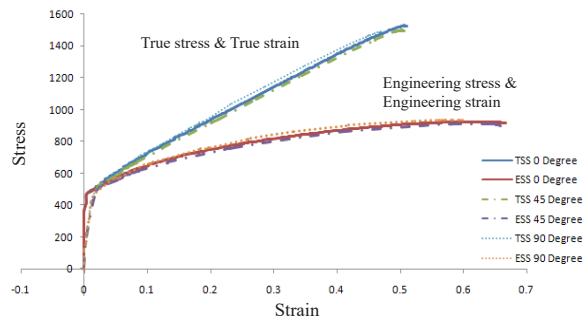

Fig. 8. *True stress-strain curve vs engineering stress strain*

True stress and true strain values, and engineering stress and strain values are plotted and are shown in Fig. 8. Based on the observed values, the Inconel 718 alloy sheet percentage of elongation and strength were found to be good in the rolling direction.

2.2 Experimental Results

A 100-ton hydraulic press and die setup shown in Fig. 9 is used for performing the hemispherical punch test and six specimens of sheet dimensions 200 mm × 200 mm, 200 mm × 180 mm, 200 mm × 160 mm, 200 mm × 140 mm, and 200 mm × 120 mm, 200 mm × 100 mm (shown in Fig. 10) are subjected to hemispherical punch test. A grid circle of Ø3 mm is marked on the specimens with an electrochemical-etching process. The specimens were clamped between the blank holder and the lower die rigidly with adequate blank holding force. Polyethylene sheet and Servo 4T 20w40 lubrication oil was applied to the sheet specimen for improving the flow of the material in hemispherical punch method. Prasad et al. [21] maintained a constant speed of 20 mm/min in the punch during stretch of specimen.

Fig. 9. *100-ton hydraulic press and die setup*

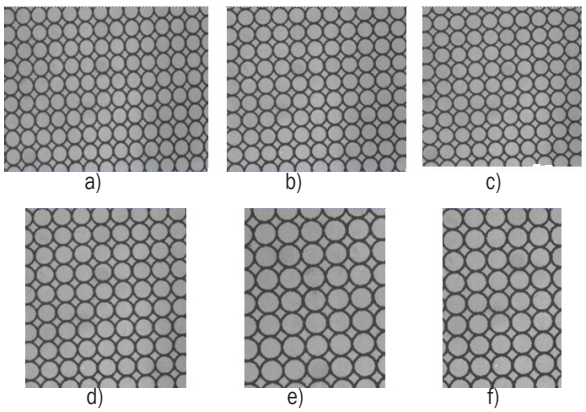

Fig. 10. *Grid printed experimental specimen before deformation, a) 200 mm × 200 mm, b) 200 mm × 180 mm, c) 200 mm × 160 mm, d) 200 mm × 140 mm, e) 200 mm × 120 mm, f) 200 mm × 100 mm*

Panickeret al. **[23]** showed that the onset of necking and failure of the specimen was monitored by a mirror mounted on the top of the die.

$$s_1 = \frac{D_1 - d_1}{D_1}, \tag{7}$$

$$s_2 = \frac{D_2 - d_1}{D_2}, \tag{8}$$

where s_1 is major strain, s_2 minor strain, D_1 is ellipse major axis distance, D_2 ellipse minor axis distance, and d_1 gird circle diameter.

Eqs. (7) and (8) are used to determine the major and minor strains by measuring the diameters of the ellipses. The minor and major strains are measured using a Dalsa Corporation machine vision system and the pixel quality is 752 × 582. The accuracy is 0.1 mm is shown in Fig. 11. The Inconel 718 alloy sheet specimens deformed are shown in Fig. 12.

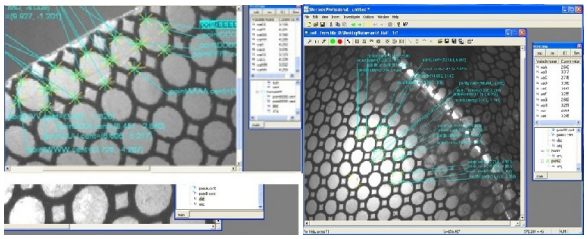

Fig. 11. *Ellipse measured by using machine vision*

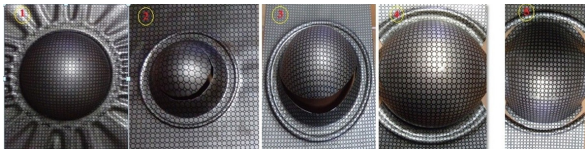

Fig. 12. *Fractured punch dome test specimen for evaluation of formability*

The FLD diagram is plotted from the measured strain values obtained from various ellipses in fracture, necked and safe regions as shown in Fig. 13. The formability is measured by FLD and the point of intersection of FLD with the true major axis value is found to be 0.34. The minor strain is observed on the left side of the FLD and major strain is observed on the right side of the FLD, which is due to biaxial expansion. The formability knowledge of Inconel 718 alloy sheet material obtained can be used in sheet metal industries for failure prediction in the design stage and for minimizing the cost incurred in the trial-and-error method. The simulated LDH values obtained from ABAQUS 6.1 and experimental LDH values measured using the coordinate measuring machine (CMM) are listed in Table 4. The simulated and experimental LDH values were in close agreement; the error percentage was found to be less than 5 %.

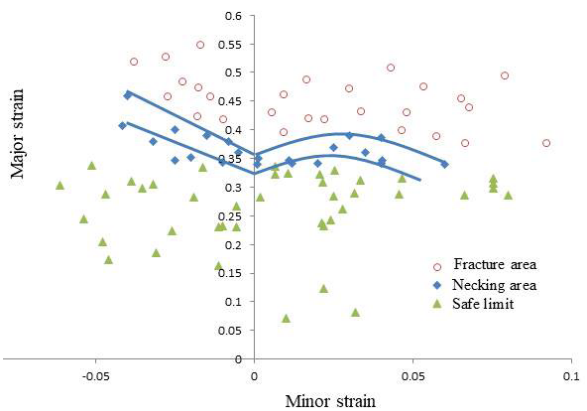

Fig. 13. *Experimental forming limit diagram of Inconel 718 alloy sheet*

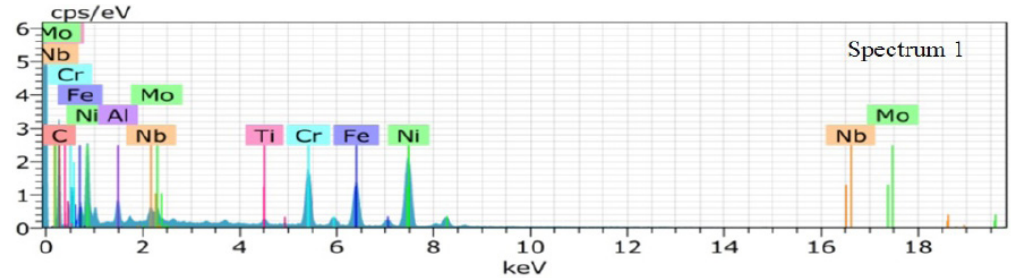

a)

Element	C K	Ni K	Fe K	Cr K	Nb K	Mo K	Ti K	Al K
Weight [%]	48.66	29.27	11.43	9.22	3.06	2.02	0.98	0.35

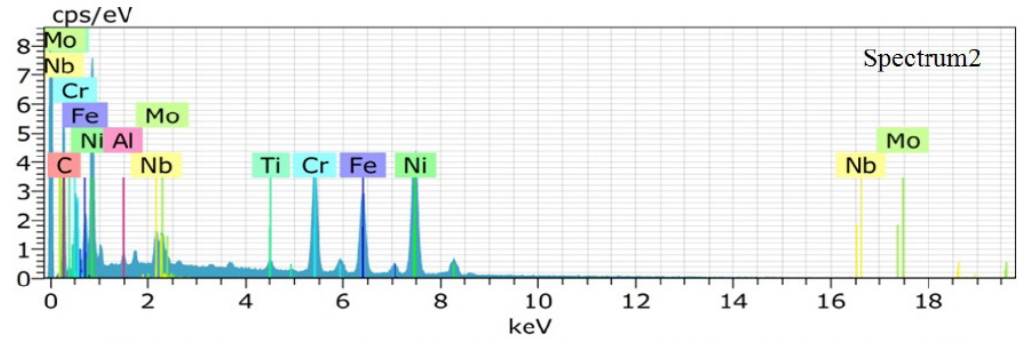

b)

Element	C K	Ni K	Fe K	Cr K	Nb K	Mo K	Ti K	Al K
Weight [%]	38.67	31.34	12.12	10.24	2.93	1.86	0.75	2.03

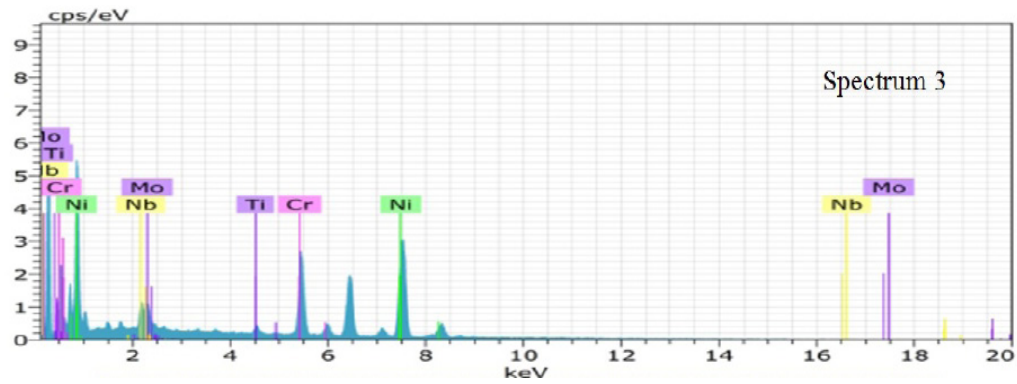

c)

Element	C K	Ni K	Fe K	Cr K	Nb K	Mo K	Ti K	Al K
Weight [%]	38.98	30.53	13.00	11.09	3.02	1.99	0.85	0.55

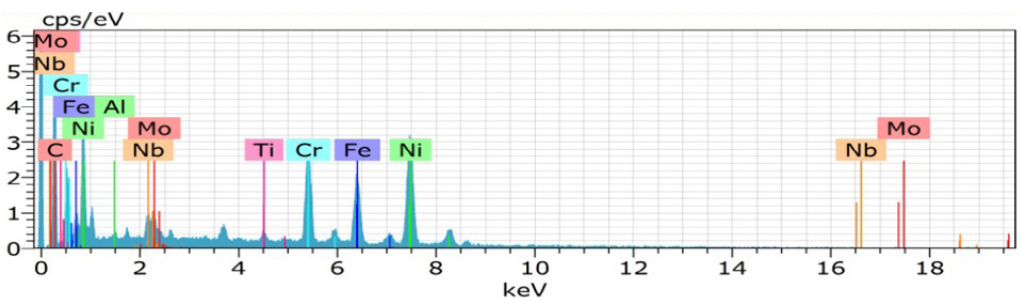

d)

Element	C K	Ni K	Fe K	Cr K	Nb K	Mo K	Ti K	Al K
Weight [%]	48.66	29.27	11.43	9.22	3.06	2.02	0.98	0.35

Fig. 14. *EDS Element analysis for fractured specimen; a) 200 mm x 100 mm, b) 200 mm x 120 mm, c) 200 mm x 140 mm, and d) 200 mm x 160 mm*

Table 4. *The simulated LDH values from ABAQUS 6.1 and experimental LDH values using the CMM*

Specimen [mm]	Simulated [mm]	Experimental (LDH) [mm]	Error [%]
200 × 100	50.65	48.6	-4.21
200 × 120	51.82	49.8	-2
200 × 140	52.25	50.2	-2
200 × 160	52.28	52.2	-0.08
200 × 180	52.83	53.2	0.69
200 × 200	53.01	53.3	0.03

2.3 Fractography Results

The features of the fracture are analysed using fractography. The fractography is performed using SEM. SEM examination of grid circle changes in the tension-tension region (right side of FLD) and tension-compression region (left side of FLD) is shown in Fig. 14. EDS analysis provides the details of the chemical composition of the enclosure in the vicinity of the fractured surface and is shown in Figs. 14a and b. The chemical compositions of materials examined at the fracture surface were similar to the composition identified in Table 1. Fractographs of 100 mm and120 mm width specimens showed minimum minor strain and maximum major strain. The shallow dimples and minimum number of voids are observed in Fig. 14a and b. The blanks were subjected to plane strain condition resulting in pure ductile failure (Fig. 14 c and d). The 140 mm and 160 mm width specimen indicated a mixed plain strain condition in the majority of the region and in the circles examined in tension-tension region. Deep dimples and more numerous voids indicate shear and ductile fracture. The 200 mm width specimen indicated no necking or failure.

Table 5. *FEA values for different specimens*

Specimen [mm]	FEA [mm]	Specimen [mm]	FEA [mm]
200 × 100	50.63	200 × 160	52.28
200 × 120	51.82	200 × 180	52.83
200 × 140	52.20	200 × 200	53.01

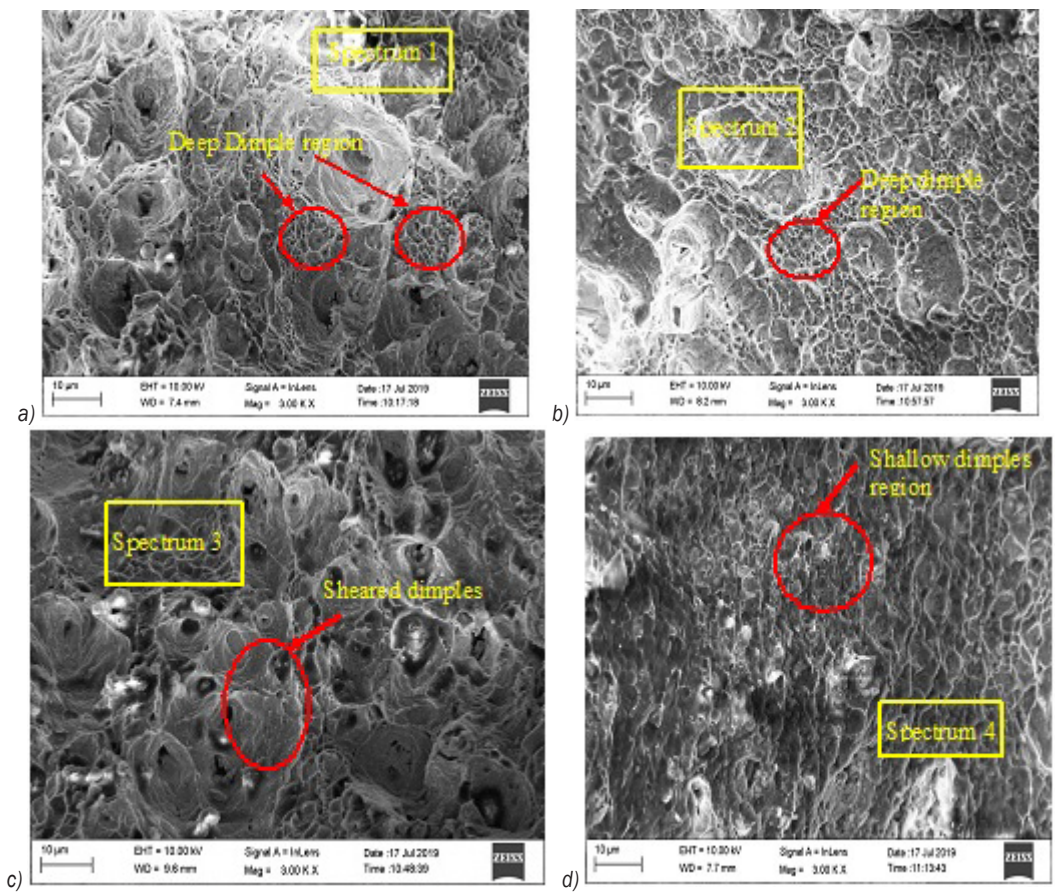

Fig. 15. *Fractographs of Inconel 718 alloy sheet specimens in hemispherical punch test; ; a) 200 mm x 100 mm, b) 200 mm x 120 mm, c) 200 mm x 140 mm, and d) 200 mm x 160 mm*

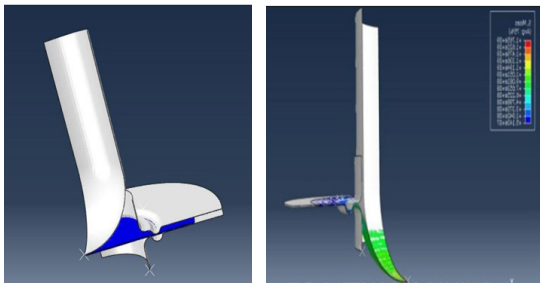

Fig. 16. *Simulated LDH values different specimens in ABAQUS 6.1*

The quarter finite element (FE) model strain distribution along the specimen is shown in Fig. 16. The detailed view of strain distribution in the Inconel 718 alloy sheet is presented in Fig. 17. FEA values are shown in Table 5.

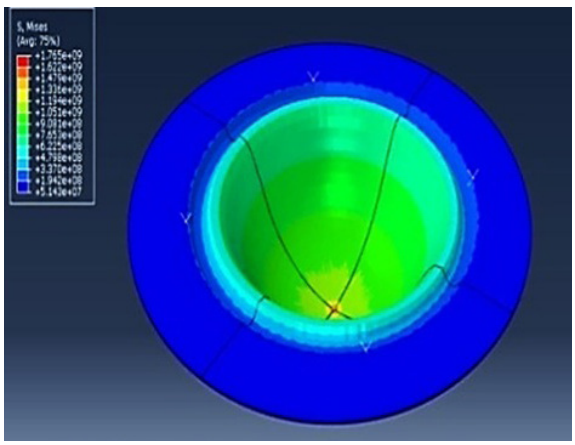

Fig. 17. *Strain distributions in Inconel 718 alloy sheet*

3 CONCLUSION

In this paper, the mechanical properties of Inconel 718 alloy sheet in longitudinal, diagonal, and traverse directions were obtained by uniaxial tensile test. Also, the LDH values of the Inconel 718 alloy sheet were examined by simulation and experimentation using a hemispherical punch method. The following are results obtained from this work.

The mechanical properties of the Inconel 718 alloy sheet of 1 mm thickness were obtained in different rolling directions. The percentage of elongation was high (47.6 %) in the rolling direction compared to other directions. The strain hardening n is found to be 0.34, which indicates good stretch ability and formability. The normal anisotropy r of 1.02 shows that material will resist thinning in drawing operation. The strength coefficient value also indicated that the material possesses good strength in the transverse direction.

Inconel 718 alloy sheet properties observed in the rolling direction were used in ABAQUS 6.1 for finite element analysis. The strain distribution in the sample dimension of 200 mm× 200 mm indicated no necking or failure in both the simulation and experimentation. The LDH values obtained from FEA and experimental results were in good agreement. The error was found to be less than 5 %. This indicates that the developed FE model can further be used to study the material behaviour of other alloy sheets numerically thereby reducing the time and cost incurred in experiments.

FLD of the Inconel 718 sheet was obtained experimentally. The strain limit obtained is the safe region in which the material is susceptible to plastic deformation without failure. As the width of the specimen increases, the material resistance to plastic deformation also increases. SEM examination of 100 mm and 120 mm width fractured sheets showed pure ductile fracture. The strain distribution in the sample dimension of 120 mm × 140 mm indicated shear ductile fracture. The presence of alloying elements before and after failure is confirmed by EDS analysis.

4 ACKNOWLEDGEMENTS

The authors are thankful to the Quality Improvement Programme (QIP), Delhi, India for proving financial support and the Department of Production Engineering, PSG College of Technology, Coimbatore, Achariya College of Engineering Technology, Puducherry, India.

5 REFERENCES

[1] Gupta, A.K., Ravi Kumar, R.D. (2006). Formability of galvanized interstitial-free steel sheets. *Journal of Materials Processing Technoogy*, vol. 172, no. 2, p. 225-237, **DOI:10.1016/j.jmatprotec.2005.10.016**.

[2] Pérez Caro, L., Schill, M., Haller, K., Odenberger, E.-L., Oldenburg, M. (2020). Damage and fracture during sheet-metal forming of alloy 718. *International Journal of Material Forming*, vol. 13, p.15-28, **DOI:10.1007/s12289-018-01461-4**.

[3] Reed, R.C. (2006). *The Superalloys Fundamentals and Applications*. Cambridge University Press, Cambridge, **DOI:10.1017/CBO9780511541285**.

[4] Anderson, M., Thielin, A.-L., Bridier, F., Bocher, P. Savoie, J. (2017). δphase precipitation in Inconel 718 and associated mechanical properties. *Materials Science and Engineering: A*, vol. 679, p. 48-55, **DOI:10.1016/j.msea.2016.09.114**.

[5] Sajun Prasad, K., Kamal, T., Panda, S.K., Kar, S., Narayana Murty, S.V.S., Sharma, S.C. (2015). Finite element validation of forming limit diagram of IN-718 sheet metal. *Materials Today:*

Proceedings, vol. 2, no. 4-5, p. 2037-2045, **DOI:10.1016/j.matpr.2015.07.174**.

[6] Banabic, D., Comsa, D.S., Eyckens, P., Kami, A., Gologanu, M. (2016). Advanced models for the prediction of forming limit curves. *Multiscale Modelling in Sheet Metal Forming*, Springer, Cham. p. 205-300, **DOI:10.1007/978-3-319-44070-5_5**.

[7] Jayahari, L., Hussaini, S.M., Dinesh Varmaa, Srividyadevi, P. (2020). Predictive study of Inconel718 mechanical properties at sub-zero temperature. *Advances in Materials and Processing Technologies*, vol. 6, no. 2, p. 233-243, **DOI:10.1080/2374068X.2020.1731234**.

[8] Djavanroodi, F., Derogar, A. (2010). Experimental and numerical evaluation of forming limit diagram for Ti6Al4V titanium and Al6061-T6 aluminium alloys sheets. *Materials and Design*, vol. 31, p.4866-4875, **DOI:10.1016/j.matdes.2010.05.030**.

[9] Narayanasamy, R., Narayanan, C.S. (2008). Forming, fracture and wrinkling limit diagram for if steel sheets of different thickness. *Materials & Design*, vol. 29, no. 7, p. 1467-1475, **DOI:10.1016/j.matdes.2006.09.017**.

[10] Badr, O.M., Rolfe, B., Hodgson, P., Weiss, M. (2015). Forming of high strength titanium sheet at room temperature. *Materials & Design*, vol. 66, p. 618-626, **DOI:10.1016/j.matdes.2014.03.008**.

[11] Toshniwal, K., Pareddy, S., Kotkunde, N., Gupta, A.K. (2017). Numerical investigation on stress based forming limit diagram for Ti-6Al-4Valloy. *Materials Today: Proceedings*, vol. 4, no. 8, p. 8096-8103, **DOI:10.1016/j.matpr.2017.07.149**.

[12] Sudarsan, C., Banker, H.K., Hazra, S., Bhagat, R., Panda, S.K. (2019). Experimental investigations on forming limit diagram of ultra-thin SS304 steel effect of circular grid size, sheet orientation, punch size and deformation speed. *Advances in Materials and Processing Technologies*, vol. 5, no. 1, p. 25-38, **DOI:10.1080/2374068X.2018.1510679**.

[13] Rahmaan,T.,Bardelcik, A., Imbert, J., Butcher, C., Worswick, M.J. (2016). Effect of strain on flow stress and anisotropy of DP600, TRIP780, and AA5182-O sheet metal alloys. *International Journal of Impact Engineering*, vol. 88, p. 72-90, **DOI:10.1016/j.ijimpeng.2015.09.006**.

[14] Li, S.L., Kang, Y.L., Zhu, G.M., Kuang, S. (2015). Effects of strain rates on mechanical properties and fracture mechanism of DP780 dual phase steel. *Journal of Materials Engineering and Performance*, vol. 24, p. 2426-2434, **DOI:10.1007/s11665-015-1495-0**.

[15] Mahalle, G., Kotkunde, N., Gupta, A.K., Singh, S.K. (2021). Efficacy of semi-empirical models for prediction of forming limit curve of IN718 alloy at elevated temperature. *Advances in Materials and Processing Technologies*, vol. 7, no. 4, p. 617-629, **DOI:10.1080/2374068X.2020.1792706**.

[16] Paul, S.K. (2012). Predicting the flow behavior of metals under different strain rate and temperature through phenomenological modeling. *Computational Material Science*, vol. 65, p. 91-99, **DOI:10.1016/j.commatsci.2012.06.039**.

[17] Paul, S.K. (2021). Control factors of forming limit curve: A review. *Advances in Industrial and Manufacturing Engineering*, vol. 2, art. ID 100033, **DOI:10.1016/j.aime.2021.100033**.

[18] Paul, S.K. (2016). Prediction of complete forming limit diagram from tensile properties of various steel sheets by a nonlinear regression based approach. *Journal of Manufacturing Processes*, vol. 23, p. 192-200, **DOI:10.1016/j.jmapro.2016.06.005**.

[19] Prasad, K.S., Panda, S.K., Kar, S.K., Sen, M., Murthy, N.S.V.S., Sharma, S.C. (2017). Microstructures, forming limit and failure analyses of Inconel718 sheets for fabrication of aerospace components. *Journal of Materials Engineering and Performance*, vol. 26, no. 4, p. 1513-1530, **DOI:10.1007/s11665-017-2547-4**.

[20] Kotkunde, N., Srinivasan, S., Krishna, G., Gupta, A.K., Singh, S.K. (2016). Influence of material models on theoretical forming limit diagram prediction for Ti-6Al-4Valloy under warm condition. *Transaction of Nonferrous Metal Society of China*, vol. 26, no. 3, p. 736-746, **DOI:10.1016/S1003-6326(16)64140-7**.

[21] Narayanasamy, R., Narayanan, C.S. (2007). Experimental analysis and evaluation of forming limit diagram for interstitial free steels. *Materials & Design*, vol. 28, no. 5, p. 1490-1512, **DOI:10.1016/j.matdes.2006.03.010**.

[22] Ravi Kumar, D., Swaminathan, K. (1999). Formability of two aluminium alloys. *Materials Science and Technology*, vol. 15, no. 11, p. 1241-1252, **DOI:10.1179/026708399101505347**.

[23] Panicker, S.S., Singh, H.G., Panda, S.K., Dashwood, R.(2015). Characterization of tensile properties, limiting strains, and deep drawing behavior of AA5754-H22 sheet at elevated temperature. *Journal of Materials Engineering and Performance*, vol. 24, p.4267-4282, **DOI:10.1007/s11665-015-1740-6**.